MEDWIN PUBLISHERS
Committed to Create Value for Researchers

Diabetes & Obesity International Journal
ISSN: 2574-7770

Modification of the Intestinal Microbiota with *Enterobacteriaceae*-specific Oligonucleotide Antimicrobials as a Novel Approach to Improve Metabolic Health

Wong N[1,2], Divekar D[1,2], Calvo TD[2], Watson A[1,2], Mayer MJ[1], McArthur M[1,2]* and Arjan Narbad[1]

[1]Quadram Institute, Norwich Research Park, UK

[2]Norwich Medical School, University of East Anglia, Norwich Research Park, UK

***Corresponding authors:** Michael McArthur, Norwich Medical School, University of East Anglia, Norwich Research Park, NR4 7UQ, UK, Tel: +44 1603 591367; Email: michael.mcarthur@uea.ac.uk

Research Article

Volume 9 Issue 2

Received Date: April 18, 2024

Published Date: August 08, 2024

DOI: 10.23880/doij-16000291

Abstract

Imbalances in the microbiota due to overgrowth of *Enterobacteriaceae* is associated with numerous metabolic conditions-most notably obesity. We describe an oligonucleotide antimicrobial, Transcription Factor Decoys (TFDs) that competitively inhibit the Crp-FNR transcription factor highly conserved amongst *Enterobacteriaceae* and is critical for the regulation of stress response and survival under anaerobic conditions. A nanoparticulate formulation delivers the TFDs to the cytoplasm of *E. coli*, as visualised by confocal microscopy, rapidly reduced viable bacteria under anaerobic conditions. *In vitro* data showed FNR TFD decreased up to $\log_{10}$ 6 CFU/ml of coliforms within the *Enterobacteriaceae* family while other families remained relatively undisturbed; similarly when delivered orally to wild-type mice *in vivo*, *Enterobacteriaceae* were significantly reduced while other key bacterial populations were unaffected. This demonstrates that TFDs can be used to make precise changes to the microbiota and has utility in testing associations between dysbiosis and disease potentially leading to the development of microbiota targeted therapeutics to tackle obesity.

Keywords: Selective Antimicrobial; Alternative to Antibiotic; Oligonucleotide Therapy; Nanomicelle; Microbiota

Abbreviations

TFD: Transcription Factor Decoys; LNP: Loaded Nanoparticles; CRP: Cyclic AMP Receptor Protein; FNR: Fumarate Nitrate Reductase.

Introduction

The human gut microbiome is a crucial organ pivotal for the health and disease [1]. Though a healthy microbiota is yet to be clearly defined, it is accepted that it consists of stable core members, is structurally robust and has large microbiological diversity [2], while diseased or dysbiotic microbiota are imbalanced and feature overgrowth of pro-inflammatory bacteria leading to functional impairment of the core microbiota [3]. This is associated with disease onset [4] such as obesity [5], type 2 diabetes melllitus (T2D) [6] and metabolic syndrome (metS) [7], that are therefore considered as interlinked conditions. As the gut microbiota carries out a multitude of functions it is a challenge to

precisely define the aetiological agent in these disease conditions but the there is a widely perceived role for the overgrowth of Enterobacteriaceae that can induce deficiency in the intestinal barrier function, leading to the leakage of bacteria and their metabolic products into the blood and concomitant chronic inflammation. This is thought to be a common mechanism explaining how gut dysbiosis affects numerous disease conditions, and emphasizes the central role of the gut-organ axes in causing multimorbidity [8]. The proinflammatory bacteria are typified by facultative anaerobes, typically *Enterobacteriaceae* that can tolerate the microanaerobic environment proximal to the intestinal epithelium, resist oxidative stress that is both typical of the ageing gut and part of macrophage defence [9]. Therefore, these species can create a niche for themselves that propgates chronic inflammation that contributes to the severity, or is causative, of metabolic diseases and so represent a novel therapeutic strategy for challenging conditions such as obesity.

Many approaches are being investigated to manipulate the gut microbiota to better understand the mechanisms of disease and identify biomarkers and new therapeutic strategies [10]. Faecal microbiota transplantation (FMT) replaces the damaged microbiotas with healthy ones, transfer from a healthy donor to a patient suffering from *C. difficile* infection (CDI) can typically restore a healthy microbiota with concomitant improvement in the condition [11,12]. Although less effective, FMT has been used to obtain long-term remission in flares of inflammatory bowel disease (IBD) such as Ulcerative Colitis (UC) [13,14]. Diet also clearly has an important effect on general microbiota structure [15], but more targeted interventions are needed to dissect the impact of bacterial outgrowths. Antimicrobial peptides that are non-toxic to the host and have a narrow-spectrum of activity are being investigated as tools to reshape the microbiota [16]. Small molecules can also have an indirect effect on microbiota composition through modulation of the immune system or interference with bacterial signaling [17,18]. Microbiome-friendly narrow spectrum antimicrobials have been mainly explored against CDI, although antibiotic e.g. fidaxomicin still found to compromise the integrity of microbiome structure and diversity [19]. Hence, the next generation of antimicrobials should be designed to be selective to protect the core microbiota, being effective against the current resistances [20] already present in the population and suppress the rise of future resistances: such a platform would allow the intelligent modification of the microbiota to improve human health.

The approach taken in this study represents a direct intervention with a predictable and tunable antimicrobial spectrum. Transcription Factor Decoys (TFDs) are effective tools to control bacterial gene expression [21] and prevent infection [22]. These are short synthetic oligonucleotides that contain the binding site for essential bacterial transcription factors. TFDs competitively inhibit these to prevent gene expression against bacterial growth. The degree of conservation of the transcription factor amongst bacterial species, and its associated binding site, determine the spectrum of the TFD antimicrobial. A TFD was designed to competitively inhibit the fumarate and nitrate reductase (FNR) transcription factor of *E. coli*, which is a homologue of the cyclic AMP receptor protein (CRP) that controls hundreds of genes involved in the switch between aerobic and anaerobic respiration and coordinates numerous virulence factors [23]. Under aerobic conditions FNR is in an inactive monomeric form, whereas in an anaerobic environment the dimerization and activation of the transcription factor is driven by formation of an oxygen-sensitive $[4Fe\text{-}4S]^{+}$ iron-sulfur cluster [24]. FNR dimers bind to their genomic consensus site 5'- TTGATnnnnATCAA-3' [25] to control expression of more than a hundred operons involved in microaerobic respiration and resistance to nitrostative stress [26]. These two functions allow these pathogens to grow in the inflamed gut epithelium of the host. The FNR transcription factor is highly conserved in *Enterobacteriaceae* and other γ-proteobacteria and so is a novel mid-spectrum agent[25] where mutants were shown to reduce growth under anaerobic conditions [27]. Delivery is achieved by forming bacterial-selective nanoparticles from a recently described bola-amphiphile, 12-bis-THA [28]. This molecule binds tightly to and condenses DNA, presumably through a combination of electrostatic forces and intercalation to form a nanoparticle that protects the TFD from degradation. This nanoparticle binds to anionic phospholipids typical of prokaryotic membranes, such as Cardiolipin [29], as part of the delivery mechanism to the bacterial cytoplasm. This study demonstrates the use of the FNR TFDs as a therapeutic tool to modify the intestinal microbiota and their potential as tools to dissect the influence of specific bacterial families in structuring intestinal microbiota.jgjghjng

Results

In vitro activity of nanoparticle TFD against *E. coli*

The TFD is a small 30 nucleotide synthetic oligonucleotide that folds to form a short double stranded fragment containing the binding site for FNR of *E. coli* [23] that is critical to the transcriptional regulation under anaerobic conditions [30]. To deliver the large and negatively charged TFD to the cytoplasm of *Enterobacteriaceae,* TFD needs to transfect the typical Gram-negative cell wall. To achieve this, the TFD was mixed with a 12-bis-THA nanoparticle to form a loaded nanoparticle (LNP). After 1.5 h of treatment incubation, *E. coli* were visualised on confocal laser scanning

microscopy where collection of images in the z-plane allowed determination of whether the TFD signal was inside of the bacterial cell as opposed to stuck to the outside. *E. coli* only control (Figure 1a) showed only the Wheat Germ Agglutinin-tetramethylrhodamine (WGA-TMR)-stained cell wall, whereas in LNP-treated *E. coli* (Figure 1b) green fluorescent TFDs were visualised within the boundaries of the WGA-TMR stained cell wall. This indicates successful TFD internalization and that the TFD is evenly distributed throughout bacterial cytoplasm.

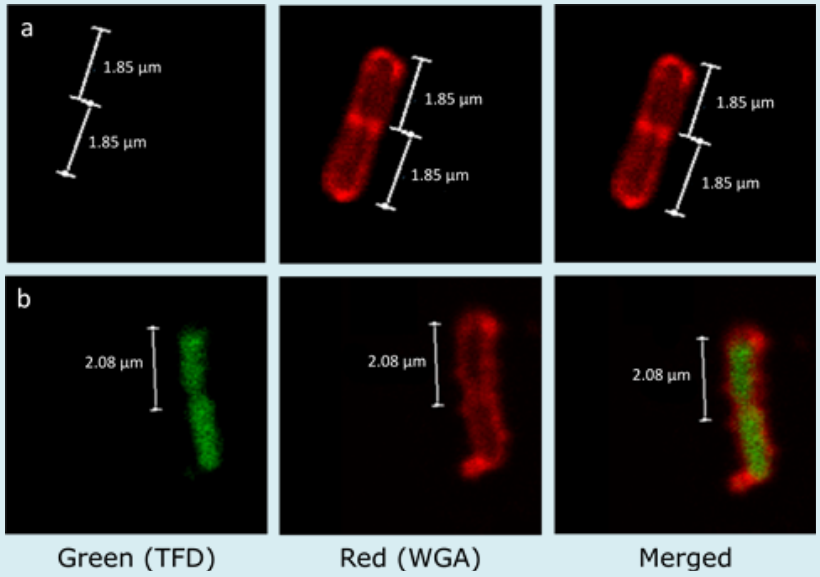

Figure 1: Biological activity against model bacterium *Escherichia coli*. Fluorescent Scanning Confocal Microscopy of *E. coli* cells either a) untreated or b) treated with loaded nanoparticles (LNPs) containing fluorescently labelled transcriptional factor decoy (TFD). The cell walls of the samples were stained with Wheat Germ Agglutinin- Tetramethylrhodamine (WGA-TMR; Red channel, middle) and the Alexa488-labeled TFD was visualised in the Green channel (left). Merged images for each sample are shown (right).

To determine the efficacy of the FNR TFD against the typical *Enterobacteriaceae* species, *E. coli*, the Minimum Inhibitory Concentration (MIC) of the LNP was measured under microaerobic conditions, where FNR become an essential regulator for bacterial survival, similar to those found proximal to the intestinal epithelium in the gut lumen. Nanoparticles containing functional TFD had a calculated MIC of 0.078 µg/ml whereas nanoparticle containing the non-functioning, scrambled TFD did not exhibit bacterial inhibition (MIC >2.5 µg/ml), suggesting TFD-specific activity against FNR. FNR LNPs have an MIC of > 24 µg/ml for other non-*Enterobacteriaceae* bacteria, suggesting FNR's antimicrobial specificity against *Enterobacteriaceae*.

Activity of nanoparticle TFD in an in vitro model of human gut microbiota.

To determine the antimicrobial effect of nanoparticles TFD in a mixture culture system, three independent studies were performed in the *in vitro* batch fermentation model with stool samples from different donors, treated with nanoparticles formed with FNR TFD (LNP), nanoparticles formed with scrambled, non-functional TFD (SLNP) or the vehicle control. The experiments were run for 8 h and the changes in microbial composition of the samples collected at 0, 0.2, 4 and 8 h were measured by both culturing on selective media and via 16S based metataxonomics. Donors were pre-screened to allow an optimal concentration to be administered, as range finding studies suggested the dose response of TFD is dependent on the starting quantities of *Enterobacteriaceae*. LNP showed significant reduction of *Enterobacteriaceae* against Control at 0.2 h and 4 h ($p<0.01$ and 0.05 respectively), while other key microbiota members e.g. *Bacteroides, Bifidobacterium, Clostridium and Lactobacillus* remained similar levels between LNP and controls (ns, $p>0.05$) at all-time points (Figure 2). This suggests LNP exert *Enterobacteriaceae*-targeted antimicrobial activity without affecting the overall bacterial population. As the media favour anaerobic growth of *Enterobactericeae* and constituted a large proportion of the microbiome, a transient reduction in total anaerobe population was observed at 4 h ($p<0.05$), which was recover at the end of experiment when TFD

activity diminished. Furthermore, preferential antimicrobial activity against *Enterobactericeae* suggested that this group is targeted far more by nanoparticles, potentially driven by interaction with the LPS layers typical of coliforms, which like Cardiolipin contains negatively charged phosphates that are expected to be the binding moiety for 12-bis-THA.

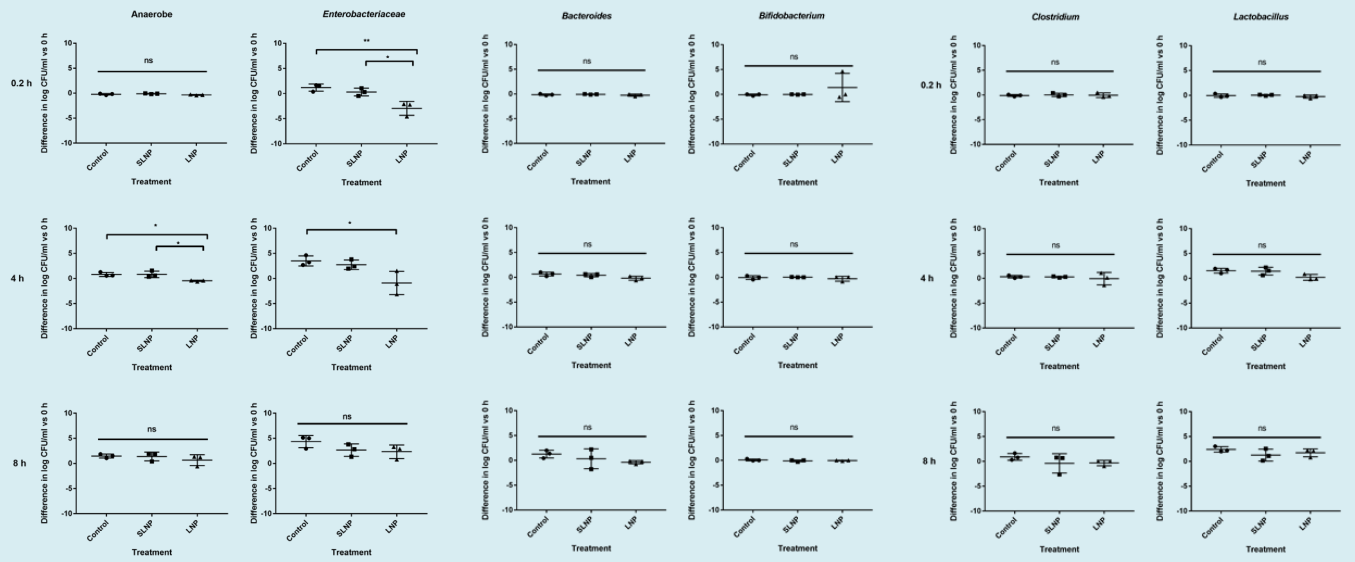

Figure 2: Changes in the viable gut microbiota community in Batch model fermentation of the human colon Samples were collected from the model and microbiological burden measured by selective plating. Samples were treated with a single dose of buffer-only as Control, LNPs loaded with the Scrambled TFD or with the active FNR TFD and assayed at 0, 0.2, 4 and 8 h. The CFU/ml of total anaerobe and coliform/ *Enterobacteriaceae* at each time point were compared to their corresponding value at 0 h from each donor. LNP significant reduced *Enterbacteriaceae* at 0.2 and 4 h with temporal reduction in anaerobe at 4 h against the controls as *Enterobacteriaceae* constitute a large proportion of the microbiome. Bacteroides, Bifidobacterium, Clostridium and Lactobacillus remain unchanged following treatment at all time points (ns, $p>0.05$). The mean of 3 biological repeats of multiple batch fermenters (each with 3 technical plating replicate) ± SD is plotted. Straight line, comparison between all treatments; pointed line, comparison between selected treatments.

To confirm the impact of TFD on live, both culturable and non-culturable bacteria from the batch fermentation, 16S metataxonomic analysis were performed with samples pretreated with propidium monoazide (PMA), which intercalates DNA in dead cells and exclude their amplification in downstream sequencing process [31], and showed a closer resemblance to the population trend to those from viable counts (data not shown). Although allocation of operational taxonomic unit (OTU) is known to skew the relative abundance in favour of the highly abundant taxa and underestimate rare taxa [32], leading to overestimation of *Enterobacteriaceae* at later time points compared to those seen from plate counts, there is a good corresponding trend to which LNP's antimicrobial activity against *Enterobacteriaceae* was observed from 0.2 and 4 h (Figure 3a) and its relative abundance were significantly reduced compared to the controls at 4 h ($p< 0.05$) (Figure 3b). Alpha diversity was investigated and no differences were seen between LNPs and the controls in terms of diversity, species richness and observed species, suggesting the administration of the TFD-loaded LNP therapy had minimal inference to the structure of the microbiome (Figure 3c). Beta diversity was analysed with weighted unifrac Principal Coordinates Analysis (PCoA), where clustering of samples observed between each time points are likely due to changes in the population as nutrients were being used in the batch fermentation model. Interestingly, LNP-treated samples consistently showed a reduced/delayed shift compared to the controls from same time point, e.g. Samples treated with LNPs at 4 h are more spatially related to all samples from the previous time point than the control treatments at 4 h, thus suggesting that LNPs may have the ability to delay structural changes exerted against the microbiome (Figure 3d).

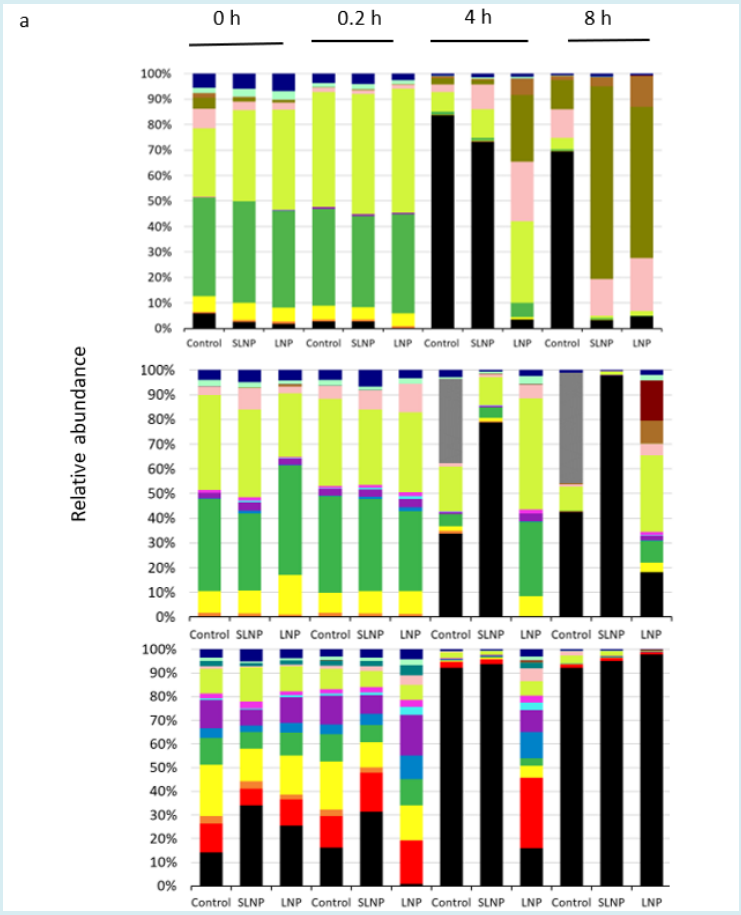

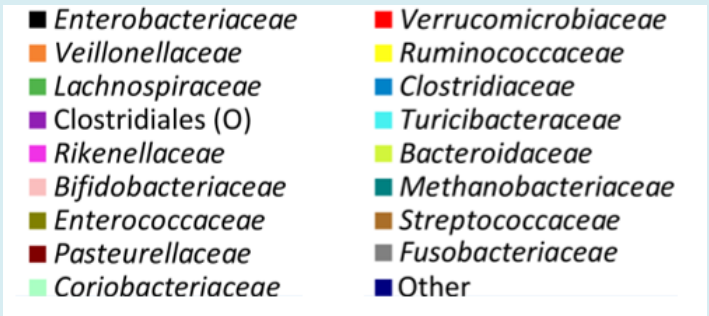

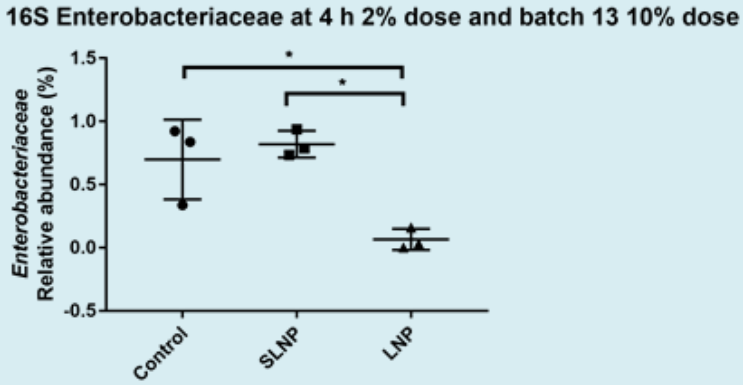

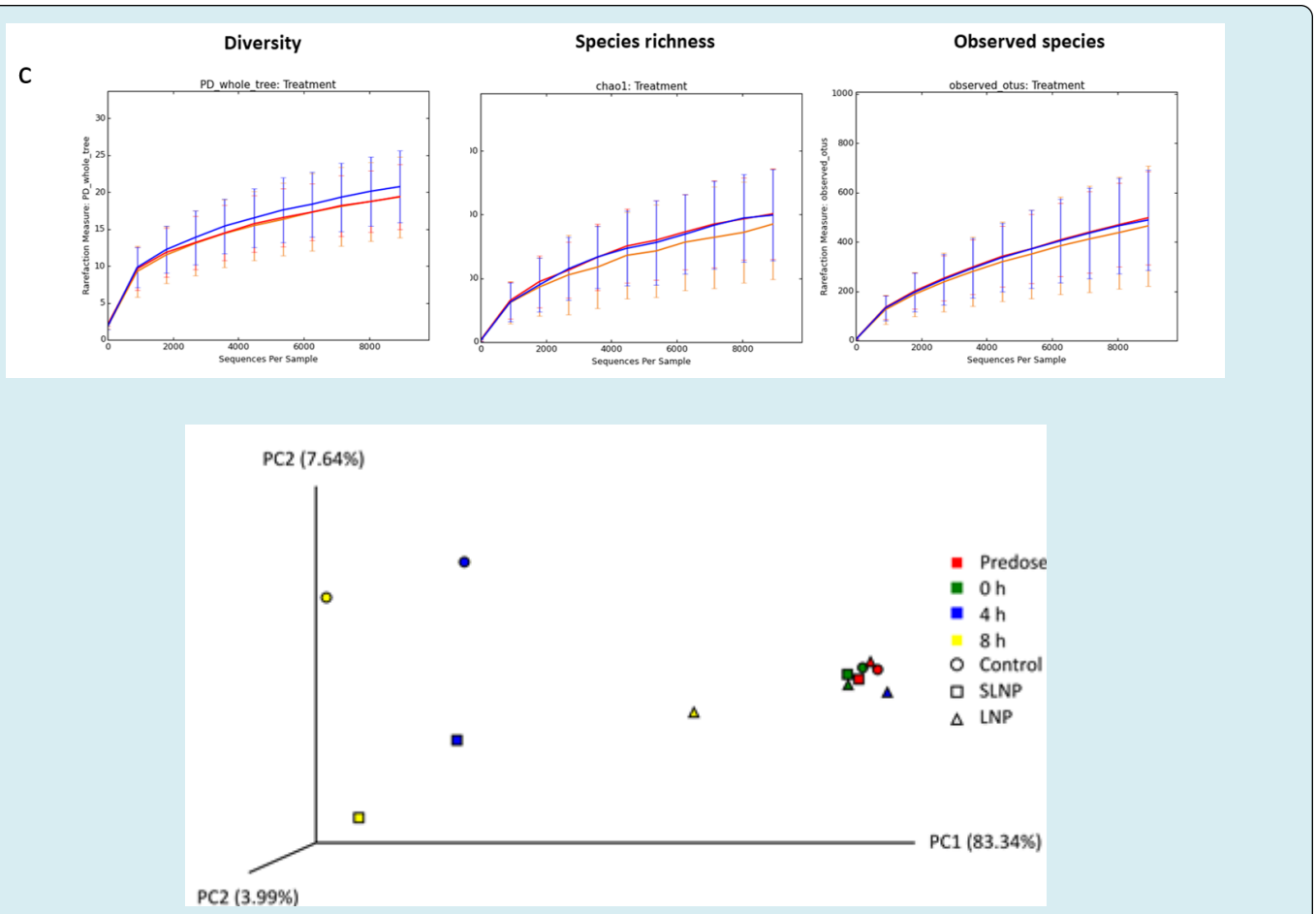

Figure 3: Analysis of Illumina sequencing data for *in vitro* batch model a) Live bacterial community analysis of 16S rRNA gene sequencing at family level for *in vitro* batch culture fermentation treated with propidium monazide. Key shows classification of bacterial families b) Relative abundance of *Enterobacteriaceae* from 16S rRNA gene sequencing at 4 h c) Alpha diversity plot showed no difference in microbiota diversity due to treatment, with Control (orange), Scrambled-TFD LNPs (blue), and LNPs with the active FNR TFD (red). Representative data from one donor was shown (see also Figure S2). D) Principal coordinate analysis (PCoA) generated from weight UniFrac analysis from a representative experiment, where x-, y- and z-axis represents the first, second and third principal coordinates respectively (see also Figure S3).

Remodeling of the murine intestinal microbiota in vivo

To determine whether nanoparticles loaded with the FNR TFD could modify the gut microbiota in an animal model, we administered LNPs to C57BL/6J mice by oral gavage. Two oral treatments of SLNP, Control or LNP (15.4 x MIC, 1.2 mg/kg) were given at 0 h and 2 h. The faecal samples were used to measure viable bacterial counts of the main bacterial populations including total anaerobes, *Bacteroides*, *Clostridium*, *Lactobacillus* and *Enterobacteriaceae* by selective plating (supplementary Figure S1). In general, while the overall anaerobe population remain relatively stable (ns, $p>0.05$), specific reduction in *Enterobacteriaceae* levels were observed at 6 h and 8 h, with levels recovering at 24 h, suggesting potential sequestration of LNPs by other bacteria (Figures 3a and b). In line with the results of the *in vitro* experiments, LNP treatment selectively decreased population of the *Enterobacteriaceae* only, with at least a $\log_{10}$ 3.1 CFU/g decrease at 6 h, where the number detected was close to the limit of detection (<333 CFU/g). Only *Enterobacteriaceae* showed any significant decrease ($p< 0.01$) in relation to the total anaerobes (Figure 3c). This suggests LNP treatment specifically reduce the viable coliform population 6 h after the initial drug administration into the stomach, without altering the viability of the rest of the gut microbiota population. A repeat of this experiment (Experiment 2) compared the previously used high dose (1.2 mg/kg) and a lower dose (0.24 mg/kg), with faecal collection performed at 8 h instead of 2 h. Again, the high

dose selectively cleared *Enterobacteriaceae* whilst leaving other bacterial families intact: relative to the control the coliform population decreased by $\log_{10}$ 2 CFU/g at 6 h and $\log_{10}$ 3.4 CFU/g at 8 h (Figure 3b), where significant decrease in *Enterobacteriaceae* in individual mice at 6 h ($p<0.01$) and 8 h ($p<0.001$) were observed compared to the Control (Figure 3d).

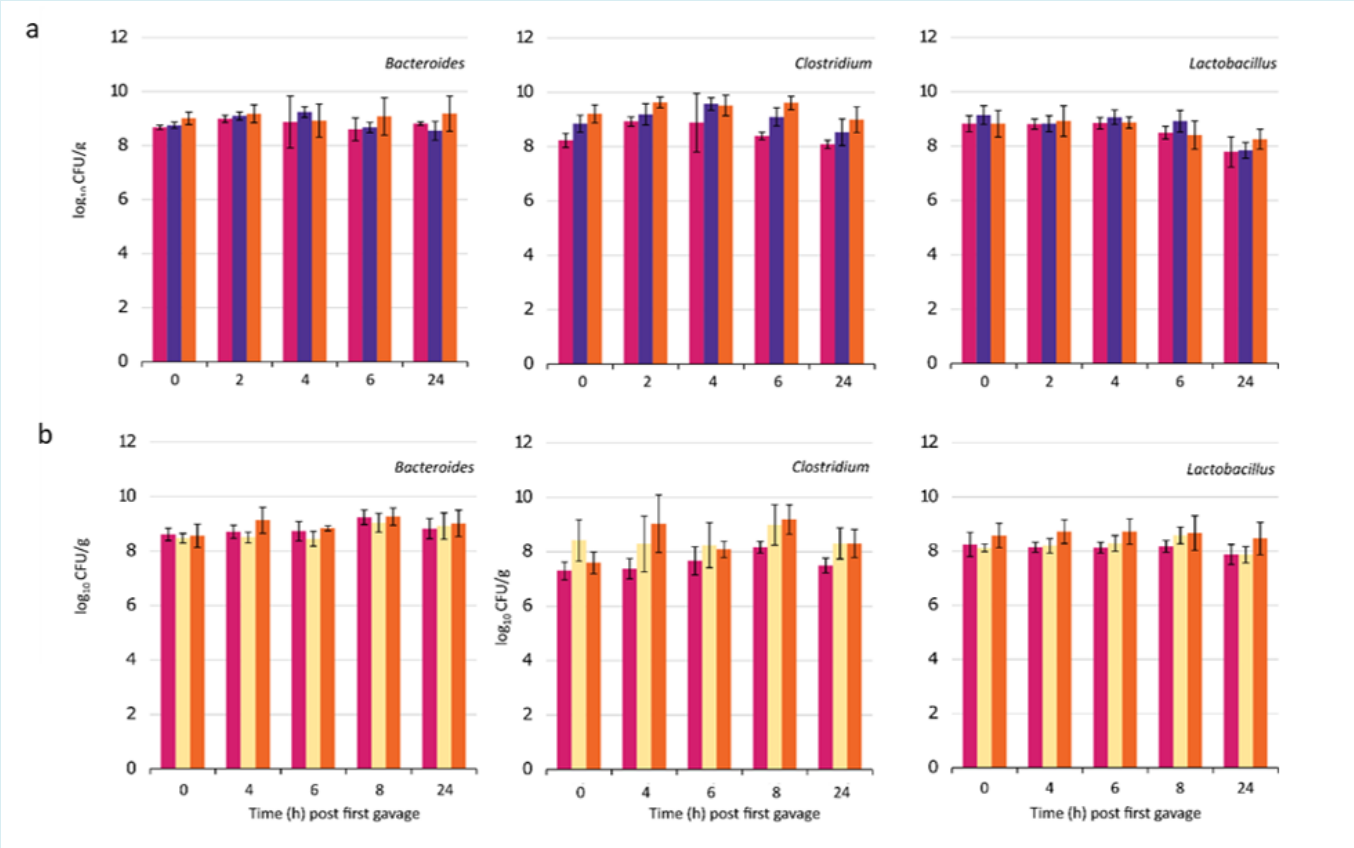

Figure S1: Bacterial viable counts for Bacteroides, Clostridium and Lactobacillus (mean ± SD) in a) mouse experiment 1, with Control (magenta), SLNP treatment (purple) and LNP treatment (orange) (both at 1.2 mg/kg). b) mouse experiment 2, with Control (magenta), low dose LNP with FNR TFD (0.24 mg/kg; yellow) and high dose (1.2 mg/kg; orange).

To determine the effect of LNP treatment on the structure of the microbiota in more detail, 16S rRNA gene community analysis was performed on samples from both *in vivo* experiments. The samples were grouped by treatments at each time point and the data shown is an average abundance of the relative number of reads for each bacterial family (Figures 4a and b). Looking at the data as a whole, large variation between samples showed no significant difference against time and treatment (ns, $p>0.05$) except shifts in family S24-7 ($P<0.05$). Looking at specific time point, significant decrease ($p<0.001$) in *Enterobacteriaceae* relative abundance were observed with LNP treatment at 6 h compared to the control (Figure 4c), implying effective antimicrobial activity immediately after the expected transit period for the drug from stomach to anus from 6 h onwards [33]. Alpha diversity showed no significant difference in the cimmunity structure as observed in chao1, observed species and PD-whole-tree with LNP treatment against the controls, when compared between treatments (Figure 4d). In addition, PCoA analysis showed no distinct clustering between treatment and time in weight for beta diversity (Figure 4e). This further implies LNP's ability to maintain the diversity, species richness and observed species of the microbiome while significantly reducing bacteria of interest.

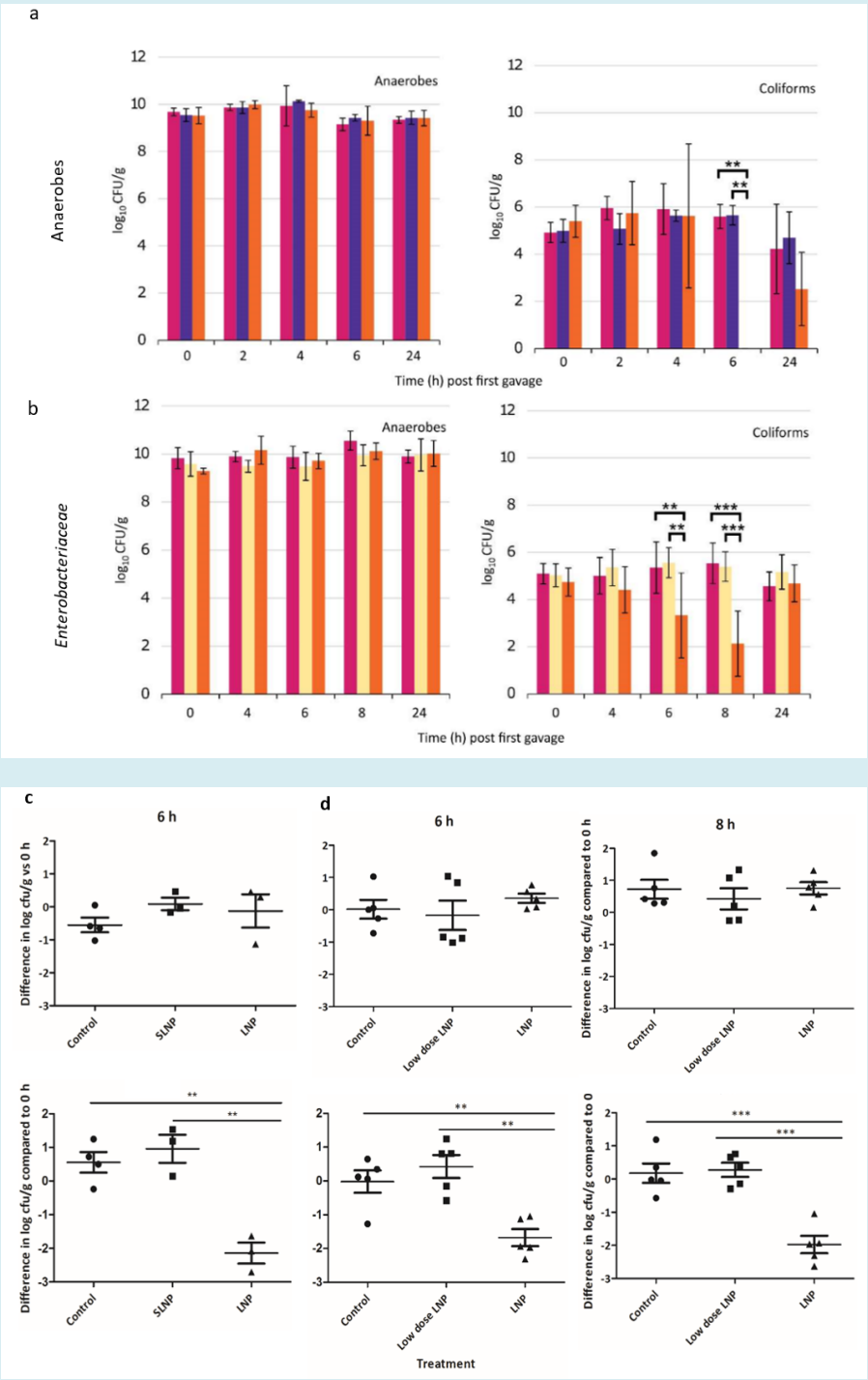

Figure 4: Microbiome analysis of mouse faecal pellets following treatment with LNPs. Bacterial viable counts for total anaerobes and Enterobacteriaceae (mean ± SD) for a) Experiment 1, with Control (magenta), scrambled LNP treatment (purple) and LNP treatment loaded with FNR TFD (orange) (both at 1.2 mg/kg). b) Experiment 2 with Control (magenta), low dose LNP (0.24 mg/kg; yellow) and high dose LNP (1.2 mg/kg; orange). For both experiments number of samples varied between 3 and 5 as animals at some time points did not produce a faecal pellet. The CFU/g of total anaerobe and coliforms at 6 h (or/and 8 h) were compared to the their corresponding value at 0 h in each mouse, statistical significance were present in Enterobacteriaceae population in c) Experiment 1 at 6 h and d) Experiment 2 at 6 and 8 h, while anaerobe population remained unchanged.

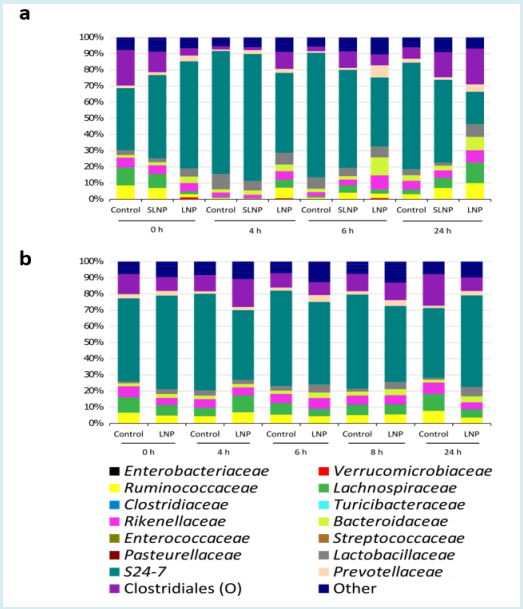

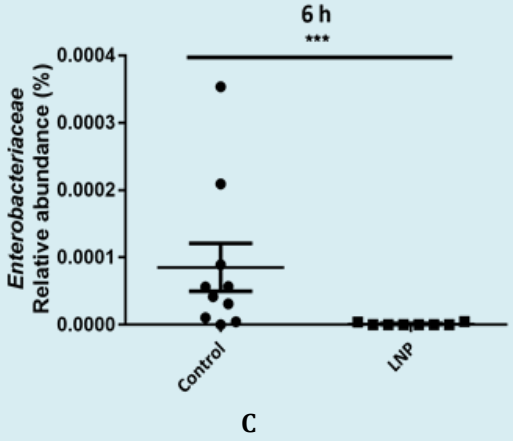

C

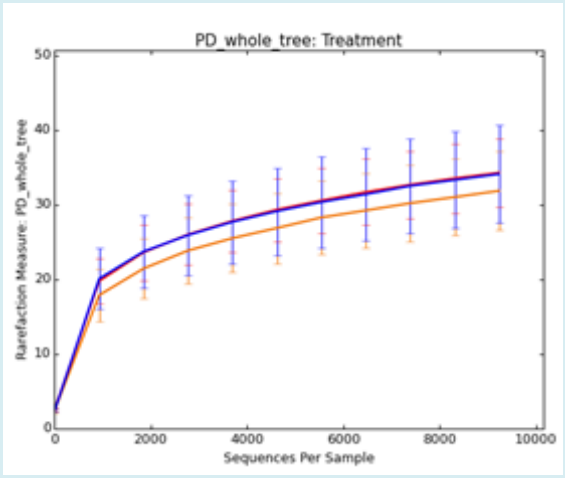

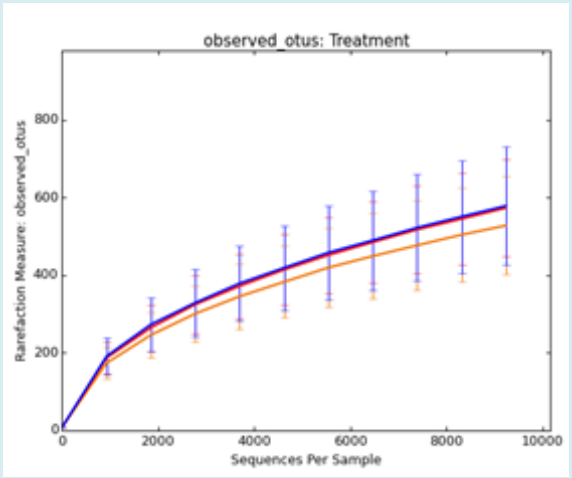

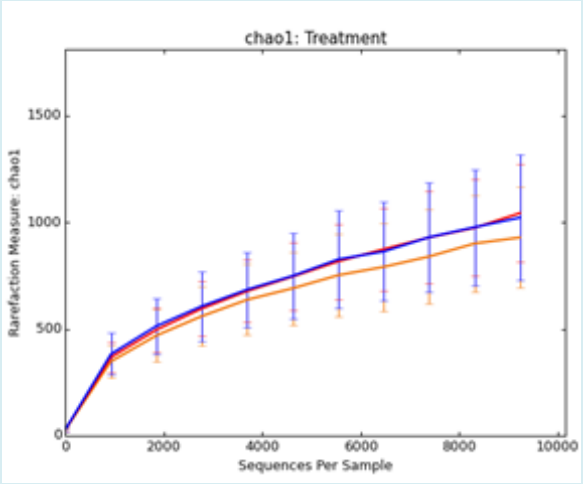

d

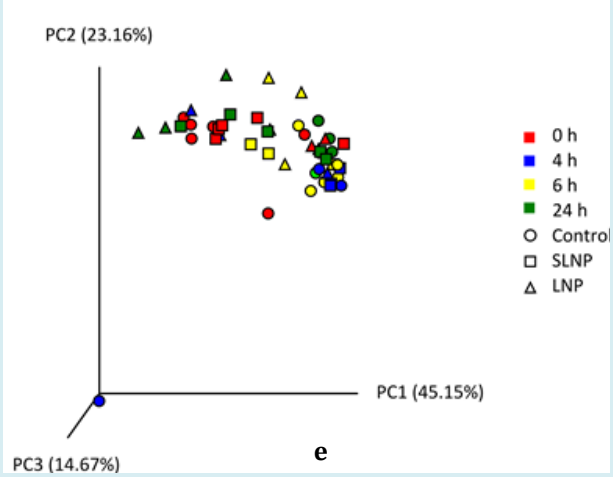

Figure 5: 16S rRNA gene analysis of live bacterial with averaged total bacterial population in a) Experiment 1 and b) Experiment 2. Key shows classification of bacterial families. c) Relative abundance of Enterobacteriaceae from 16S rRNA gene sequencing. Scatter plot data were presented as mean ± SEM. Double and triple asterisks denote $P \leq 0.01$ and $P \leq 0.001$ respectively. d) Alpha diversity plot showed no difference in microbiota diversity due to treatment, with Control (orange), Scrambled-TFD LNPs (blue), and LNPs with the active FNR TFD (red) (see supplementary Figure S5). e) Principal coordinate analysis (PCoA) generated from weight UniFrac analysis from a representative experiment, where x-, y- and z-axis represents the first, second and third principal coordinates respectively (See supplementary Figure S6).

Mice were observed throughout the experimental period to monitor early indicators of health. To establish whether treatment with the effective doses (1.2 mg/kg) of nanoparticles affect the epithelial barrier, sections of the gastrointestinal tract from euthanised mice were compared with those unaffected by high dose of nanoparticles and from Control animals. Haemotoxylin and eosin staining were performed to assess whether epithelial damage occurred in the intestine and representative histological samples are shown in Figure 5. In control mice, duodenum, jejunum, ileum and colon showed normal histological morphology similar to those seen in LNP-treated mice. The lamina propria appears normal and intact, with no signs of inflammations or cell shedding. Normal crypt architecture, no observable inflammatory cell infiltration and no muscle thickening were seen, goblet cell depletion was absent, as were crypt abscess, indicating no histological damage typical of colitis [34]. Observations of stress e.g. hunchback posture and piloerection were alleviated in the second study by omitting faecal pellet collection following oral gavage at 2 h, as opposed to 10% of mice reaching humane endpoints when treated with LNP or SLNP in the first study, suggesting this may be linked to a combination of possible side effects from nanoparticles and the experimental set up which get exacerbated under stressful situations. Nanoparticles are being reformulated to reduce potential negative effects for future studies.

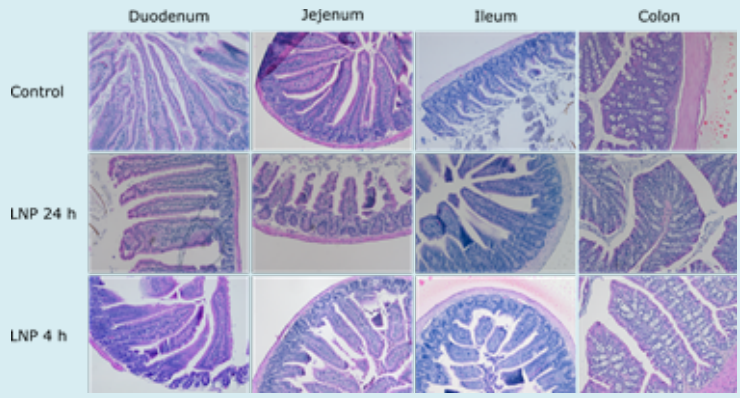

Figure 6: Histological photomicrograph of mouse intestine stained with haematoxylin and eosin at 10x magnification from saline control mouse; LNP-treated healthy mouse at 24 h; and LNP-treated mouse euthanised at 4 h after the start of experiment.

Discussion

An oligonucleotide (FNR-TFD) with mid-spectrum antimicrobial activity against *Enterobacteriaceae* was shown to predictably remove certain members of the intestinal microbiota. The oligonucleotide formulated as a nanoparticle was able to efficiently transfect the model *E. coli* species and had high potency. An *in vitro* batch fermentation model of the human intestinal microbiota confirmed the spectrum of this TFD, as *Enterobacteriaceae* were selectively removed whilst leaving other bacterial families unaffected as measured by selective bacterial plating and 16S rRNA gene analysis. Batch model fermentation have been shown to increase growth of *Enterobacteriaceae* [35] as the experiment progresses, we have use this to demonstrate TFD's ability to inhibit growth of the rapidly dividing *Enterobacteriaceae* in a complex community setting. Being a selective antibacterial therapy, dose efficacy will largely depend on the levels of target organisms present in the individual, fine tuning between the dosing regimen and the *Enterobacteriaceae* level could enhance and prolong of antimicrobial activity in different donors, and to avoid unnecessarily high dose rendering non-specific NP effects. Plate counting results showed that the last batch fermentation donor had 7 log instead of 6 log of *Enterobacteriaceae*, and constituted >30% as opposed to <5% of the relative abundance from 16S metataxonomic analysis. This likely account for why a 5x therapeutic dose was required to observe a similar antimicrobial effect than the other donors. To investigate whether this novel treatment could predictably modify the murine intestinal microbiota *in vivo,* a total dose of 1.2 mg/kg of the LNPs significantly suppressed growth of *Enterobacteriaceae* after the transit period of 6-8 h ($p < 0.001$) again with no significant changes in structure and diversity of the microbiota. Previous studies showed that the antibiotics norfloxacin and ampicillin both significantly decreased *Enterobacteriaceae* levels by $\log_{10}$ 6 CFU/g of faeces [36], however other gut commensal bacteria were also disrupted due to lack of selectivity. Additionally, most mouse studies only evaluate antimicrobial activity after 24 h [37-39]. The fast acting nature of LNP demonstrated here may be advantageous to reduce rapidly multiplying pathogenic bacteria, particularly at the start of an infection. We only dosed the mice twice and it is anticipated that increasing dose numbers would serve to keep *Enterobacteriaceae* numbers low.

Following treatment with TFD in this study the gut microbiota composition of the gut commensal bacteria was not altered significantly over the 24 h period with significant compensational changes in only one family group as opposed to several in another pathogen-selective treatment when *Enterobacteriacae* declined [37], showing that TFD therapy is less disruptive and show compositional recovery at a much quicker rate. Our results suggest that the TFD technology has strong potential in specifically modulating the microbiota for other health and disease association studies or as a bespoke suppressor of a selected group in the microbiota in a fast acting setting. Selectively remove *Enterobacteriaceae* can also be used to establish to what extent the gut microbiota is a contributory factor in inflammatory conditions underpinning obesity and related metabolic diseases such as T2D and metS. Proof of principle in selectively inhibiting specific members of the gut microbiome as demonstrated here provides a route to developing a narrow spectrum antimicrobial that targets *Enterobacteriaceae* by preventing their growth in inflamed tissue, which should correct dysbiosis and reduce inflammatory response. In future such targeted approach has potential for addressing other microbiota-associated disorders [40-42].

Methods

Preparation of TFD nanoparticles

The oligonucleotides used in this study were manufactured and purified by HPLC at Integrated DNA Technologies (Belgium). The TFD used is the FNR TFD and has the sequence 5'-T*T*T*T*GATCCAAATCAA-Teg-TTGATTTGGATC*A*A*A-3' [23], where asterisks denote a phosphorothioate linkage and -Teg- denotes an internal tetraethyleneglycol linker. Two versions were prepared, with and without a 5' Alexa-Fluor 488 dye molecule to allow imaging. A scrambled version of the FNR TFD was also prepared that contained the same nucleotides and maintained secondary structure but destroyed the FNR binding site and has the sequence: 5'-A*C*A*TTCAAGCTAATT-Teg-AATTAGCTTGAA*T*G*T-3'. The TFDs were resuspended in ultra-pure water at a concentration of 0.25 mg/mL, then incubated for 5 min at 95°C and let to cool to room temperature to allow the complementary sequences, which contain the binding site for FNR, to anneal. The TFD was stored at -20°C until needed.

12-bis-THA.I was prepared as described elsewhere [43]. Briefly, The bolamphiphile 1,1'-(dodecane-1, 12-diyl)bis(9-amino-1,2,3,4-tetrahydroacridinium) iodide [12-bis-THA I] was synthesised by Shanghai Chempartner Co., LTD. with final purity 95 %. Briefly, a mixture of 1,2,3,4-tetrahydroacridin-9-amine and the 1,12-diiododecane (2:1 molar ratio) was stirred at 155°C for 5h, then cooled down. The crude product was triturated with 90% ethanol (ethanol: deionized water, V:V = 90:10) for 3 times at reflux to get the iodide salt of the desired compound. Ion exchange of 12-bis-THA iodide with chloride was carried out using chloride form of Dowex resin (16-100 mesh) from Sigma-Aldrich previously conditioned with HCl 5% in order to achieve replacement of the iodide with chloride, as previously reported in the literature. Briefly, Dowex resin was washed on a Buchner

funnel with Milli-Q water (1 L), then it was conditioned with HCl 5% (0.5L) and rinsed again with water Milli-Q until neutral pH had been achieved. Additionally washing was continued until no chloride precipitation from the eluate was detected following treatment with $AgNO_3$. Finally the resin was thoroughly washed with methanol (1L). Following the activation of the resin, 12-bis-THA iodide (100 mg, 0.12 mmol) was dissolved in methanol (100-120 mL) and mixed with Dowex (10 g of wet resin in methanol). The mixture was left stirring at room temperature overnight, then it was filtered under pressure through a buchner (size 4). The dispersion of 12-bis-THA with iodide counter ion in aqueous solution was obtained by dissolving the compound in DMSO at 10 mg/mL and then diluting in 50 mM MES buffer (pH 5.5) with 0.1% (v/v) hydroxypropyl methylcellulose (HPMC) and vortexed to give a homogenous dispersion with a final concentration of 150 µg/ml. As these nanoparticles formed in the absence of TFD they are referred to as empty nanoparticles and to form TFD-loaded nanoparticles (LNPs) the oligonucleotide was added to the MES buffer at a concentration of 10 µg/ml and mixed.

Assessing antimicrobial activity of LNPs in vitro

The Minimum Inhibitory Concentration (MIC) of the LNPs was determined against the *E. coli* reference strain ATCC 25922 by the broth dilution method using anaerobic conditions [44]. Modified M9 minimal media, M9 supplemented with 40 mM lactose, 40 mM sodium fumarate, 1 mM $MgSO_4$, 0.1 mM $CaCl_2$ plus 10% LB broth, was inoculated with 5 x 10^5 CFU/mL ATCC 25922. Bacteria were grown with a serial dilution of LNPs at 37°C for 24 h under anaerobic conditions and extent of growth measured by reading absorbance at 600 nm.

Confocal laser scanning microscopy

E. coli cells were grown to mid-log growth (Optical Density of 0.2 to 0.3 at 630 nm) in Luria Bertani (LB) broth. Fresh culture was mixed with an equal volume of LNPs prepared with Alexa-Fluor488 (λ ex488/em519) labelled oligonucleotide, resulting in a final concentration of the encapsulating agent (12-bis-THA) of 90 µM, and incubated at room temperature for a total of 1.5 h, under constant agitation in the dark. For the final 30 mins the bacterial membrane was labelled with a fluorescent membrane dye, in the case of *E. coli* WGA-TMR (λ ex555/em580 nm, Life Technologies, UK) at a final concentration of 10 µg/ml. The samples were smeared onto poly-L-lysine coated slides (Sigma-Aldrich, UK) and incubated for a further 30 min in the dark at room temperature. Slides were then gently washed with filter-sterilized PBS and air dried. Mounting media (Fluoroshield, Sigma-Aldrich, UK) was added to the smears and coverslips applied. Microscopy slides were kept in the dark at 4°C prior to analysis by confocal microscopy using a Leica SP5 confocal microscope and image processing performed with the software package Image-J (NIH Image).

Batch culture fermentation

Batch culture fermentation were performed using a method described previously [45] under anaerobic conditions. Batch culture medium contained: Peptone (2 g/l), yeast extract (2 g/l), NaCl (0.1 g/l), K_2HPO_4 (0.04 g/l), KH_2PO_4 (0.04 g/l), $MgSO_4.7H_2O$ (0.01 g/l), $CaCl.2H_20$ (0.01 g/l), $NaHCO_3$ (2 g/l), Tween 80 (0.002% v/v), vitamin K (5 x 10^{-6}% v/v), cysteine. HCl (0.5 g/l), bile salts (0.5 g/l) and Hemin (0.02 g/l). 10 g/l glucose was added to the autoclaved media before use as a carbon source. Batch culture media (135 ml) was reduced by overnight stirring in a nitrogen atmosphere in the batch fermentation vessels. These were connected to water jackets filled with 37°C water for temperature control and a pH of 6.8 was maintained with an automated pH control system. Freshly voided faecal samples were diluted 1:10 in pre-reduced PBS and placed into a Seward stomach bag, before being homogenised at 230 rpm for 45 s using the Seward Stomacher 400 circulator. 15 mL of the resulting faecal slurry was added to each of the vessels. LNPs or vehicle controls were added to the faecal inoculum according to the prescreened *Enterobacteriaceae* concentration (3 µg/ml and or 15 µg/ml). Samples were taken at 0 h (before addition of treatments, 0.2 h, 4 h, 8 h for viable colony counts, and DNA extraction for downstream 16S rRNA gene sequencing.

Viable bacterial cell counting

Agar plates and all relevant apparatus and reagents were pre-reduced in the anaerobic cabinet overnight before use. Faecal slurries were serially diluted in PBS and plated at each dilution in triplicates under anaerobic conditions. The colony forming units (CFU) were calculated using the formulation: CFU/ml = no. of colonies x dilution factor / volume plated.

Total anaerobes (Wilken Chalgren) and coliforms (MacConkey no. 3) (including *Bacteroides*, *Clostridium*, *Lactobacillus*, *Enterobacteriaceae* and *Bifidobacterium* in supplementary figures) were enumerated with media agar as previously described [35] and incubated at 37°C for 24 h.

Phylogenetic analysis of bacterial communities using 16S rRNA gene sequencing

Samples obtained from batch culture fermentation vessel was centrifuged at 5000 g for 15 min at 4°C and resuspended in 500 µl of pre-reduced PBS. To obtain viable bacteria for downstream sequencing, an aliquot of 1.25 µl of Propidium monoazide (PMA) (20 mM) (Biotium) intercalating dead bacterial DNA [46] was mixed with each sample in a 1.5 ml

Eppendorf and incubated on a shaker at 195 rpm in the dark for 5 min at room temperature. PMA photoactivation was performed on a Phast blue light apparatus (GenIUL) for 15 min. The sample pellet were obtained by centrifugation at 10000 g for 8 min and genomic DNA was extracted using the Fast DNA SPIN kit for soil (MP Biomedicals) according to manufacturer's instruction, with three bead-beating steps of 1 min each [47]. DNA was stored at -20°C before analysis.

Bioinformatic analysis of 16S rRNA gene sequencing

Paired-end 16S community sequencing was performed using the Illumina Miseq platform by the Earlham Institute (Norwich, UK) targeting the 16S small subunit V4 rRNA region. Quantitative Insights Into Microbiological Ecology (QIIME) was used to analyse the bacterial community [48]. Forward and reverse reads of the samples were joined and sequences were filtered so that the sequences are between 200 bp and 1000 bp using prinseq lite. Other criteria included having an average quality score of at least 25 within a 50 bp length, read length between 200 and 1000 bp, and having an Illumina quality digit of >0. Chimeric sequences were detected and eliminated using Usearch 6.1 [49] and prinseq-lite [50]. Greengenes 13.8 was used to assign bacterial taxonomy among phylum to species level from the operational taxonomic units, also enabling reverse strands to be searched against the Greengenes database by uclust, with the confidence value of 50% as threshold and OTU clustered from trimmed reads at 97% identity level. Chao1, observed otus and PD whole tree were used to calculate rarefraction plots and alpha diversity. Beta-diversity PCoA plots were generated by weighted and unweighted Unifrac distances and visualised in the Emperor tool [48]. An average sequencing depth of 71455 and 144665 reads per sample were obtained from batch culture fermentation experiments and *in vivo* mouse model respectively.

Modification of murine intestinal microbiota

Wild type C57BL/6J mice littermates were bred and caged at the Disease Monitoring unit (University of East Anglia, Norwich) until 8 weeks old before the experiment commenced. All experiments were performed under Home Office project licence PDADA1B0C in accordance with intuitional guidelines. Faecal pellets were collected 3 days before the start of experiment to record baseline *E. coli* levels. On the day of the experiment, 100 µl of LNPs were administered using oral gavage tubes (Linton Instrumentation) at each time point according to the dosing regimen; faecal pellets were collected for viable bacterial plate counting and 16S rRNA gene sequencing as described above.

When the experiment ended at 24 h, mice were euthanised and dissected. Intestinal tissues were collected and stored at 4°C or further analysis. Wax-embedded tissue sections were stained by haematoxylin and eosin before analysis on Olympus BX60 microscope to determine the presence of intestinal cell shredding and inflammation.

Statistical analysis

Our primary hypothesis was that the effect of LNP's antimicrobial activity against *Enterobacteriaceae* would be evident at 6 and 8 hours. Change scores from time 0 to 6 (or 8) hours were calculated for each mouse by subtracting the log CFU/g value at 0 h from the value at 6 (or 8) h. Log transformation was used to stabilise variances across groups and ensure normal distribution of scores within groups. One way ANOVA and tukey multiple comparison test was used to compare the change scores across treatment groups, with the threshold for statistical significance set at $p<0.05$. 16S Group significance against time and treatment were analysis using Bonferroni test within Qiime. To analyse relative abundance from 16S rRNA gene sequencing, one-tailed Mann Whitney test was performed. P- values denoted throughout the article is described below.

Symbol	Meaning
ns	$P > 0.05$
*	$P \leq 0.05$
**	$P \leq 0.01$
***	$P \leq 0.001$
****	$P \leq 0.0001$

Table 1: P- Values.

Acknowledgements

The author(s) gratefully acknowledge the support of the Biotechnology and Biological Sciences Research Council (BBSRC); this research was funded by the BBSRC Institute Strategic Programme Gut Microbes and Health [BB/R012490/1] and the iCASE PhD studentship [BB/KO12940/1]. We thank Justin O'Grady for his assistance with the application of PMA, and Lee Kellingray for technical assistance with the use of the colon model.

The research was conducted in compliance with the Project License under the animals (scientific procedures) act 1986, and adheres to the principles set forth in the Guide for Care and Use of Laboratory Animal under Home Office guidance. The colon model study that used human samples was approved by the Quadram Institute Bioscience Human Research Governance Committee (IFR01/2015), and London - Westminster Research Ethics Committee (15/LO/2169).

References

1. Tremaroli V, Backhed F (2012) Functional interactions between the gut microbiota and host metabolism. Nature 489: 242-249.

2. McBurney MI (2019) Establishing What Constitutes a Healthy Human Gut Microbiome: State of the Science, Regulatory Considerations, and Future Directions. The Journal of nutrition 149(11): 1882-1895.

3. Cammarota G (2015) The involvement of gut microbiota in inflammatory bowel disease pathogenesis: Potential for therapy. Pharmacology & Therapeutics 149: 191-212.

4. Stecher B, Maier L, Hardt WD (2013) 'Blooming' in the gut: how dysbiosis might contribute to pathogen evolution. Nature reviews Microbiology 11: 277-284.

5. Gonzalez-Muniesa (2017) Obesity. Nat Rev Dis Primers 15: 17034.

6. Patra D (2023) Recent insights of obesity-induced gut and adipose tissue dysbiosis in type 2 diabetes. Frontiers Molecular Biology 10: 1224982.

7. Saltier AR, Olefsky JM (2017) Inflammatory mechanisms linking obesity and metabolic disease. J Clin Invest 127(1): 1-4.

8. Anand S, Mande SS (2022) Host-microbiome interactions: Gut-Liver axis and its connection with other organs. NPJ Biofilms Microbiome 8: 89.

9. Walter J, Armet AM, Finlay BB, Shanahan F (2020) Establishing or Exaggerating Causality for the Gut Microbiome: Lessons from Human Microbiota-Associated Rodents. Cell 180(2): 221-232.

10. Belcheva A, Irrazabal T, Martin A (2015) Gut microbial metabolism and colon cancer: Can manipulations of the microbiota be useful in the management of gastrointestinal health? BioEssays : news and reviews in molecular, cellular and developmental biology 37: 403-412.

11. Bakken JS (2011) Treating Clostridium difficile infection with fecal microbiota transplantation. Clinical gastroenterology and hepatology 9(12): 1044-1049.

12. Kellingray L (2018) Microbial taxonomic and metabolic alterations during faecal microbiota transplantation to treat Clostridium difficile infection. The Journal of infection 77(2): 107-118.

13. Bennet JD, Brinkman M (1989) Treatment of ulcerative colitis by implantation of normal colonic flora. Lancet 1(8630): 164.

14. Shi Y (2016) Fecal Microbiota Transplantation for Ulcerative Colitis: A Systematic Review and Meta-Analysis. PloS one 11: e0157259.

15. David LA (2014) Diet rapidly and reproducibly alters the human gut microbiome. Nature 505: 559-563.

16. Gebhart D (2015) A Modified R-Type Bacteriocin Specifically Targeting Clostridium difficile Prevents Colonization of Mice without Affecting Gut Microbiota Diversity. mBio 6(2): e02368-14.

17. Rasko DA (2008) Targeting QseC signaling and virulence for antibiotic development. Science (New York, N.Y.) 321(5892): 1078-1080.

18. Rooks MG (2016) QseC inhibition as an antivirulence approach for colitis-associated bacteria. Proceedings of the National Academy of Sciences of the United States of America 114(1): 142-147.

19. Ajami NJ, Cope JL, Wong MC, Petrosino JF, Chesnel L (2018) Impact of Oral Fidaxomicin Administration on the Intestinal Microbiota and Susceptibility to Clostridium difficile Colonization in Mice. Antimicrobial agents and chemotherapy 62(5): e02112-17.

20. Paterson DL, Bonomo RA (2019) Multidrug-Resistant Gram-Negative Pathogens: The Urgent Need for 'Old' Polymyxins. Adv Exp Med Biol 1145: 9-13.

21. McArthur M, Bibb MJ (2008) Manipulating and understanding antibiotic production in Streptomyces coelicolor A3(2) with decoy oligonucleotides. Proceedings of the National Academy of Sciences of the United States of America 105(3): 1020-1025.

22. Marín-Menéndez A (2017) Antimicrobial Nanoplexes meet Model Bacterial Membranes: the key role of Cardiolipin. Scientific reports 7: 41242.

23. Korner H, Sofia HJ, Zumft WG (2003) Phylogeny of the bacterial superfamily of Crp-Fnr transcription regulators: exploiting the metabolic spectrum by controlling alternative gene programs. FEMS microbiology reviews 27(5): 559-592.

24. Sutton VR, Mettert EL, Beinert H, Kiley PJ () Kinetic analysis of the oxidative conversion of the [4Fe-4S]2+ cluster of FNR to a [2Fe-2S]2+ Cluster. Journal of bacteriology 186(23): 8018-8025.

25. Matsui M, Tomita M, Kanai A (2013) Comprehensive computational analysis of bacterial CRP/FNR superfamily and its target motifs reveals stepwise

evolution of transcriptional networks. Genome biology and evolution 5(2): 267-282.

26. Cole JA (2018) Anaerobic Bacterial Response to Nitrosative Stress. Advances in microbial physiology 72: 193-237.

27. Kargeti M, Venkatesh KV (2017) The effect of global transcriptional regulators on the anaerobic fermentative metabolism of Escherichia coli. Mol Biosyst 13(7): 1388-1398.

28. Mamusa M, Sitia L, Barbero F, Ruyra A, Calvo TD, et al. (2017) Cationic liposomal vectors incorporating a bolaamphiphile for oligonucleotide antimicrobials. Biochimica et biophysica acta 1859(10): 1767-1777.

29. Marín-Menéndez A, Montis C, Díaz-Calvo T, Carta D, Hatzixanthis K, et al. (2017) Antimicrobial Nanoplexes meet Model Bacterial Membranes: the key role of Cardiolipin. Scientific reports 7:41242.

30. Ni J, Hatori S, Wang Y, Li YY, Kubota K (2019) Uncovering Viable Microbiome in Anaerobic Sludge Digesters by Propidium Monoazide (PMA)-PCR. Microbial ecology 79(4): 925-932.

31. Kembel SW, Wu M, Eisen JA, Green JL (2012) Incorporating 16S gene copy number information improves estimates of microbial diversity and abundance. PLoS computational biology 8(10): e1002743.

32. Padmanabhan P, Grosse J, Asad AB, Radda GK, Golay X (2013) Gastrointestinal transit measurements in mice with 99mTc-DTPA-labeled activated charcoal using NanoSPECT-CT. EJNMMI research 3(1): 60.

33. Kim JJ, Shajib MS, Manocha MM, Khan WI (2012) Investigating intestinal inflammation in DSS-induced model of IBD. Journal of visualized experiments 1(60): 3678.

34. Avendano G, Nueno-Palop C, Narbad A, George SM, Baranyi J, et al. (2015) Interactions of Salmonella enterica subspecies enterica serovar Typhimurium with gut bacteria. Anaerobe 33: 90-97.

35. Membrez M, Blancher F, Jaquet M, Bibiloni R, Cani PD, et al. (2008) Gut microbiota modulation with norfloxacin and ampicillin enhances glucose tolerance in mice. FASEB journal 22(7): 2416-2426.

36. Yao J, Carter RA, Vuagniaux G, Barbier M, Rosch JW, et al. (2016) A Pathogen-Selective Antibiotic Minimizes Disturbance to the Microbiome. Antimicrobial agents and chemotherapy 60(7): 4264-4273.

37. Spees AM, Wangdi T, Lopez CA, Kingsbury DD, Xavier MN, et al. (2013) Streptomycin-induced inflammation enhances Escherichia coli gut colonization through nitrate respiration. mBio 4(4): e00430.

38. Lackraj T, Ohnson-Henry K, Sherman PM, Goodman SD, Segall AM, et al. (2016) Novel antimicrobial peptide prevents C. rodentium infection in C57BL/6 mice by enhancing acid-induced pathogen killing. Microbiology (Reading, England) 162(9): 1641-1650.

39. Salzman NH, Jong HD, Paterson Y, Harmsen HJM, Welling GW, et al. (2002) Analysis of 16S libraries of mouse gastrointestinal microflora reveals a large new group of mouse intestinal bacteria. Microbiology (Reading, England) 148(Pt 11): 3651-3660.

40. Steegenga WT, Mischke M, Lute C, Boekschoten MV, Pruis MGM, et al. (2014) Sexually dimorphic characteristics of the small intestine and colon of prepubescent C57BL/6 mice. Biology of sex differences 5: 11.

41. Zákostelská Z, Málková J, Klimešová K, Rossmann P, Hornová M, et al. (2016) Intestinal Microbiota Promotes Psoriasis-Like Skin Inflammation by Enhancing Th17 Response. PloS one 11(7): e0159539.

42. Mamusa M, Resta C, Barbero F, Carta D, Codoni D, et al. (2016) Interaction between a cationic bolaamphiphile and DNA: The route towards nanovectors for oligonucleotide antimicrobials. Colloids and surfaces. B, Biointerfaces 143: 139-147.

43. Lambden PR, Guest JR (1976) Mutants of Escherichia coli K12 unable to use fumarate as an anaerobic electron acceptor. J Gen Microbiol 97(2): 145-160.

44. Mandalari G, Palop CN, Tuohy K, Gibson G, Bennett R, et al. (2007) In vitro evaluation of the prebiotic activity of a pectic oligosaccharide-rich extract enzymatically derived from bergamot peel. Applied microbiology and biotechnology 73: 1173-1179.

45. Chieh-Hsien L, Sih-Rong W, Jen-Chieh P, Ramireddy L, Yu-Cheng C, et al. (2016) Designing primers and evaluation of the efficiency of propidium monoazide – Quantitative polymerase chain reaction for counting the viable cells of Lactobacillus gasseri and Lactobacillus salivarius. Journal of Food and Drug Analysis 25(3): 533-542.

46. Kellingray L, Tapp HS, Saha S, Doleman JF, Narbad A, et al. (2017) Consumption of a diet rich in Brassica vegetables is associated with a reduced abundance of sulphate-reducing bacteria: A randomised crossover study. Molecular nutrition & food research 61(9): 1600992.

47. Kuczynski J, Stombaugh J, Walters WJ, González A, Caporaso JG, et al. (2012) Using QIIME to analyze 16S rRNA gene sequences from microbial communities. Current protocols in microbiology.

48. Edgar RC (2010) Search and clustering orders of magnitude faster than BLAST. Bioinformatics 26(19): 2460-2461.

49. Schmieder R, Edwards R (2011) Quality control and preprocessing of metagenomic datasets. Bioinformatics 27(6): 863-864.